Proton versus neutron excitations in the high-spin spectrum of ^{102}Cd

K. P. Lieb, D. Kast, A. Jungclaus, and I. P. Johnstone*

II. Physikalisches Institut, Universität Göttingen, Bunsenstrasse 7-9, D-37073 Göttingen, Germany

G. de Angelis, C. Fahlander,[†] and M. de Poli

Istituto Nazionale di Fisica Nucleare, Laboratori Nazionali di Legnaro, I-35020 Legnaro, Italy

P. G. Bizzeti

Istituto Nazionale di Fisica Nucleare, Sezione di Firenze, I-50125 Firenze, Italy

A. Dewald, R. Peusquens, and H. Tiesler

Institut für Kernphysik, Universität zu Köln, D-50937 Köln, Germany

M. Górska[‡] and H. Grawe

Gesellschaft für Schwerionenphysik, D-64291 Darmstadt, Germany

Using the reaction ^{58}Ni(^{50}Cr,α $2p$) and the coincidence recoil distance Doppler shift technique, we determined picosecond lifetimes of high-spin states in ^{102}Cd. The positive-parity yrast and yrare cascades evidence the competition and interplay of the two proton holes in the $g_{9/2}$ orbit and four neutrons in the $d_{5/2}$, $g_{7/2}$, and $h_{11/2}$ orbits, outside the $Z=N=50$ ^{100}Sn core. At positive parity, this interplay leads to multiplets of states in the spin range 6^+–10^+, some of which are connected by very weak $E2$ transitions. At higher spins, spin-aligned proton holes and neutrons lead to magnetic rotation. Energies and transition strengths when compared with the predictions of several shell model calculations reveal the high sensitivity on the model parameters.

I. INTRODUCTION

Having 48 protons and 54 neutrons, the transitional nucleus ^{102}Cd is close enough to the doubly magic ^{100}Sn that its structure may be expected to follow the shell model. On the other hand, it has a sufficiently large number of valence nucleons to possibly develop collective features, similar to the heavier vibrational-like Cd isotopes. As both protons and neutrons can occupy high-angular momentum orbits, i.e., $\pi(g_{9/2})$ and $\nu(g_{7/2}, h_{11/2})$, the properties of the high-spin states should reflect the competition and interplay of both types of particles. Indeed, recent in-beam γ-ray work [1–4], in which the yrast sequence was established up to spin 19 $\hbar$, evidenced typical multiplets of states at intermediate spins, which appear to arise from just this competition between proton holes and neutron particles. In particular, the magnetic dipole and the electric quadrupole moment of the 8^+ yrast state, $g=+1.29(3)$ and $Q=87(10)$ e fm^2, unambiguously determine the $\pi^{-2}(g_{9/2})$ two-proton-hole structure of this state. From the extremely retarded $E2$ strength of few mW.u. for the $8^+\rightarrow6^+$ yrast transition, Alber *et al.* [1] concluded that the 6^+ yrast state is a rather pure two-particle neutron excitation. The distinct pattern of either proton *or*

neutron excitations at low spins is expected to develop, at higher spins, into a situation where both types of spin-aligned particles contribute to the total angular momentum, giving rise to magnetic rotation. However, due to the complexity of the level scheme and the lack of firm spin-parity assignments and absolute transition strengths, this interpretation of the high-spin spectrum is still very tentative [4].

II. EXPERIMENTAL DETAILS

In this paper, we present measurements of transition strengths which are the result of a recoil distance Doppler shift lifetime experiment carried out by means of the reaction ^{58}Ni(^{50}Cr,α $2p$)^{102}Cd. The 205-MeV ^{50}Cr beam was provided by the XTU tandem accelerator at the INFN at Legnaro. The plunger apparatus [5] consisted of a 1.2 mg/cm^2 stretched ^{58}Ni foil and a 12.3-μm thick, parallel Au stopper foil. Data were taken at 12 flight distances ranging from 16 μm to 7 mm. The recoil velocity was $v/c=3.4(1)\%$, relative to the velocity of light. The γ radiation was detected in the GASP array in close geometry [6], containing a total of 40 Compton-suppressed Ge detectors. Details of the plunger apparatus, the spectrometer, and the coincidence data taken and their analysis are described in the recent ^{104,105}In lifetime study by Kast *et al.* [7]. The majority of lifetimes was obtained using the differential decay curve method (DDCM) [8,9]. This method is very suitable in the case of delayed cascade and/or side feedings typical of irregular shell model level structures populated in heavy-ion fusion reactions. By measuring the intensities of the stop or flight peak components, I_{out}^S and I_{out}^F, of the decay γ ray, with a gate set on the

---

*Permanent address: Physics Department, Queens University, Kingston, Canada.

[†]Also at: Division of Cosmic and Subatomic Physics, Lund University, Lund, Sweden.

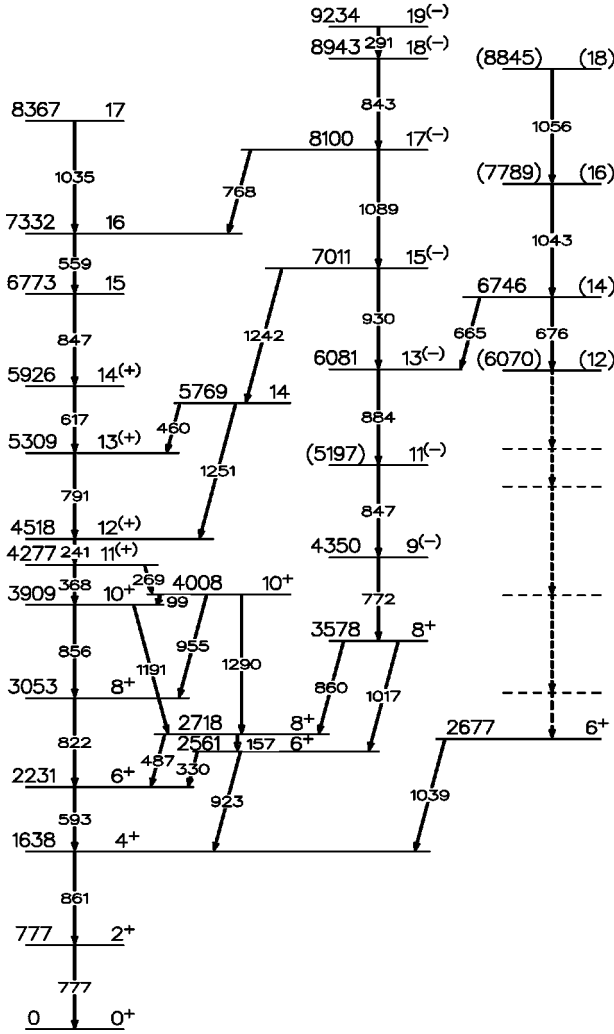[‡]Present address: Katholieke Universiteit Leuven, B-3300 Leuven, Belgium.

FIG. 1. High-spin states in ^{102}Cd taken from Refs. [1–4]. The positive parity of states above spin 10 is based on the present lifetime measurements. The ordering of the sequence of γ rays connecting the 2677-keV 6^+ state and the 6746-keV (14) state is tentative [4].

flight component γ_{in}^F of a sufficiently strong direct feeder transition, one obtains the level lifetime $\tau=I_{out}^S/(dI_{out}^F/dt)$.

III. EXPERIMENTAL RESULTS

The published level scheme carrying the predominant γ-ray flux and including the parity assignments made in the present work is shown in Fig. 1 and will be briefly discussed below. As examples of the DDCM lifetime measurements of four prominent transitions, Fig. 2 illustrates the γ-ray intensities I_{out}^S and (dI_{out}^F/dt) and the lifetime values τ deduced from them, as a function of the flight distance. Note that the 0.4-ps lifetime of the 5309-keV state, which marks the lower limit of the present plunger experiment, has not been corrected for Doppler shift attenuation as discussed by Petkov *et al.* [9]. Problems in the analysis occurred in the determination of the lifetimes of the 2_1^+, 4_1^+, and 8_2^+ levels, because the flight peaks of the strong feeder transitions of 856 and 861 keV fully overlap among themselves and with that of the 860-keV $8_2^+\rightarrow 8_1^+$ transition (see Fig. 1) and therefore could not be used as individual DDCM gates. In addition, there occur strong 861- and 592-keV lines in the nucleus ^{101}Ag populated in the reaction ^{58}Ni(^{50}Cr,α $3p$)^{101}Ag [10]. In the case of the 8_2^+ state, the value $\tau(10_1^+)=1.8(6)$ ps obtained for the 1191-keV transition, was inferred into the analysis of the 822-keV transition gated with the 368-keV $11^{(+)}\rightarrow 10^+$ flight peak and led to the lifetime $\tau(8_2^+)=4.5(10)$ ps. A less favorable situation occurred for the 2^+ and 4^+ yrast states for which only the upper limits of their lifetimes could be determined as $\tau(2^+)$, $\tau(4^+)<8.1$ ps, by considering the 777-keV $2^+\rightarrow 0^+$ transition and gating on the flight peak of the 593-keV feeder transition of the 4^+ level. Upper lifetime limits were also accessible in the case of the presumed negative-parity states at 6746, 7789, 8100, and 8943 keV (see Fig. 1), by gating on the 291- and 1056-keV flight peaks and looking at the 1089- and 676-keV transitions, respectively. Gating on the 843- and 1056-keV flight peaks was not possible, due to the multiplet structures of these lines.

The measured lifetimes and deduced reduced transition strengths are summarized in Table I. It is noteworthy that most $M1$ strengths are of the order of 0.1–1.5 Weisskopf
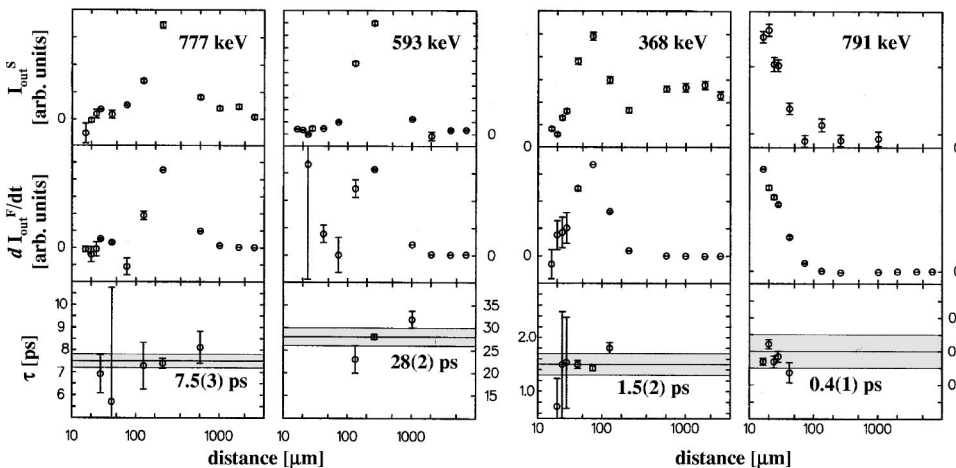

FIG. 2. Variations of the stop peak component I_{out}^S and the slope of the flight peak component dI_{out}^F/dt, of several transitions in ^{102}Cd, gated with the flight peak component γ_{in}^F of the corresponding feeder transitions. The lower parts illustrate the deduced lifetime values τ and their average values.

TABLE I. Lifetimes and transition strengths in ^{102}Cd.

State [a]		Lifetime		Transition		
E_x (keV)	I^π	τ(ps)	E_γ(keV)	Branching ratio (%)	Multipolarity	Reduced transition strength (W.u.) [e]
777	2^+	<8.1[b]	777	100	$E2$	>12.5
1638	4^+	<8.1[b]	861	100	$E2$	>7.5
2231	6^+	28(2)	593	100	$E2$	14(1)
2718	8_1^+	56(4)ns[f]	487	42(2)	$E2$	$5.9(5)\times10^{-3}$
			157	58(2)	$E2$	1.8(2)
3053	8_2^+	4.5(10)	822	100	$E2$	17(4)
			492	<5	$E2$	<14
3909	10_1^+	1.8(6)	1191	23(2)	$E2$	2.1(7)
			856	61(2)	$E2$	24(8)
4008	10_2^+	0.9(2)	1289	60(2)	$E2$	5.5(12)
			955	23(1)	$E2$	9.3(21)
			198	10(1)	$M1$	1.5(3)
			99	6(1)	$M1/E2$	0.43(10)
4277	$11^{+\ c}$	1.5(2)	368	44(2)	$M1/E2$	0.18(3)
			269	56(2)	$M1/E2$	0.59(3)
4518	$12^{+\ c}$	2.5(2)	241	100	$M1/E2$	0.87(8)
5309	$13^{+\ c}$	0.4(1)	791	100	$M1/E2$	0.16(4)
5926	$14^{+\ c}$	2.2(2)[d]	617	100	$M1/E2$	>0.06
6746	$14^{(-)}$	<8[b]	676	44(2)	$E2$	>11
			665	25(2)	$M1/E2$	$>3\times10^{-3}$
7789	$16^{(-)}$	<8[b]	1043	100	$E2$	>2.9
8100	$17^{(-)}$	<1.8[b]	1089	70(2)	$E2$	>7.3
			768	17(1)	$E1$	$>9\times10^{-5}$
8845	$18^{(-)}$	2.6(2)[d]	1056	100	$E2$	>7.8
8943	$18^{(-)}$	<1.8[b]	843	76(2)	$M1/E2$	>0.02
9234	$19^{(-)}$	2.3(2)[d]	291	100	$M1/E2$	>0.50

[a]From Refs. [1–4] and present work.
[b]Upper lifetime limit.
[c]Parity assignment from present work.
[d]Effective lifetime.
[e]In the case of mixed $M1/E2$ transitions, a mixing ratio of $\delta=0$ was assumed. The strengths were corrected for internal conversion.
[f]From Ref. [1].

units (W.u.) and therefore rather large. As an important result of the present study, the short lifetimes of the yrast states above the 10^+ level rule out any change of parity and determine the stretched $M1$ character of the upper transitions in this cascade. Although no lifetimes have been obtained for the states above the 5926-keV $14^{(+)}$ level in this cascade, it is most probable (and in agreement with the results of the shell model calculations presented below) that all these states have positive parity, too. Such sequences of stretched, strong $M1$ transitions (shears mode) have been interpreted as arising from magnetic or antimagnetic rotation [11,12]. Among the $E2$ strengths we find moderate ones in the 10–25-W.u. range, which are typical for nuclei of this mass region having several valence nucleons [13,14], but also smaller ones around 1 W.u., besides the very weak $8_1^+\rightarrow6_1^+$ transition mentioned before.

IV. INTERPRETATION AND CONCLUSIONS

Two sets of shell model calculations of the level structure and transition strengths in ^{102}Cd were carried out, in addition to those published in Refs. [2,4]. In the first calculation ($SM1$), which was performed by means of the program RITSSCHIL [15], we adopted a model space of ten protons ($=2$ proton holes) in the $g_{9/2}$ and $p_{1/2}$ orbits and four neutrons in the $d_{5/2}$, $s_{1/2}$, $d_{3/2}$, $g_{7/2}$, and $h_{11/2}$ orbits, outside the ^{88}Sr (^{100}Sn) core. Their single-particle energies and effective two-body matrix elements were taken from Ref. [13]. The effective single-particle $E2$ charges were chosen in accordance with all our previous calculations, $e_\pi=1.72e$, $e_\nu=1.44e$. For calculating the $M1$ strengths, we used quenched single-particle g factors of the spin part, $g_{\pi,\nu}^s=0.7g_{\pi,\nu}^s(sp)$. As has been discussed in our recent work on ^{104,105}In and ^{94}Ru [7,16,17], the large number of neutrons in
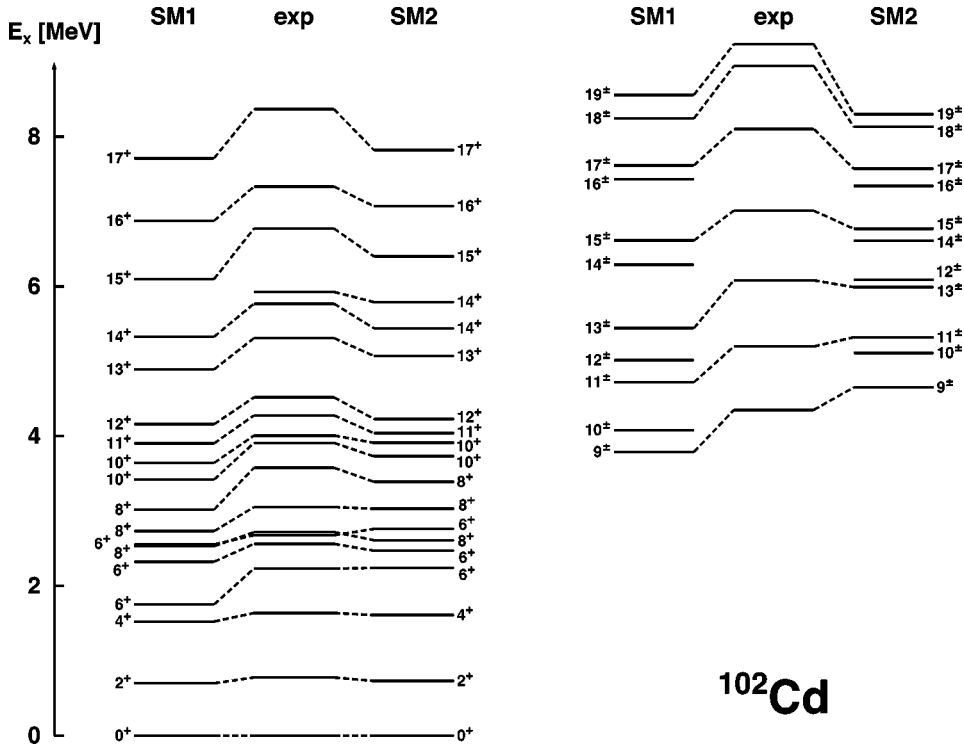
FIG. 3. Comparison of the experimental high-spin level scheme of ^{102}Cd with the calculations $SM1$ and $SM2$ described in the text.

^{102}**Cd**

so many orbits poses a certain problem, especially concerning the neutrons in the $h_{11/2}$ orbit. As the spin range of the present study is far below the maximum value $I^{\pi}=24^{+}$, which can be reached with the $[\pi^{-2}(g_{9/2})_8\nu^4(h_{11/2})_{16}]$ partition, we restricted the number of $h_{11/2}$ neutrons to a maximum of two for positive parity and one for negative parity, respectively. Proton excitations across the $N=50$ shell gap were neglected for reasons discussed in the recent work on lifetimes and magnetic moments in ^{94}Ru and ^{95}Rh by Jung-claus and co-workers [16,17].

In Fig. 3, the calculated level scheme $SM1$ with up to two $h_{11/2}$ neutrons is compared with the experiment and the result of the precision calculation by Schubart *et al.* [2]. The correct level sequence is reproduced, although the theoretical spectrum is somewhat compressed. The $SM1$ calculations pose the 6^+ yrast state too low, but do rather well for the energies of the 8^+ and 10^+ yrast and yrare states. As expected there was only a small shift of the theoretical levels with and without considering the $h_{11/2}$ neutrons, which evidently contribute very little at low spins. The negative-parity yrast sequence is lowered by about 500 keV. In Table II and Fig. 4 the calculated transition strengths are compared with the experimental numbers and for the $E2$ transitions up to the 8_1^+ state with the predictions of Persson *et al.* [4]. As to the level structure in the spin range 10^+-14^+, the calculation reproduces fairly well the large $M1$ strengths, although it overemphasizes the ratio of the $11^+\rightarrow10_2^+$ and $11^+\rightarrow10_1^+$ strengths, which experimentally is 3.5 and theoretically 75. At high spins, the strong $M1$ transitions are the consequence of the underlying seniority $\nu=4$ or 6 partitions $[\pi^{-2}(g_{9/2})_8\nu^{2,4}(d_{5/2},\,g_{7/2})]$ which are also listed in Table II. Indeed, 60–80 % of the wave functions of the yrast states at spins $10_2^+-14^{(+)}$ have this nature and therefore determine

this structure as being a magnetic rotation. The calculations predict a similar sequence of states at negative parity and a very large $M1$ strength of 1.8 W.u. for the $19^{(-)}\rightarrow18^{(-)}$ transition, based on the predominant partition $[\pi^{-2}(g_{9/2})_{6,8}\nu^3(d_{5/2},\,g_{7/2})\nu(h_{11/2})]$ in both states.

While the calculation $SM1$ is rather successful for the states in which proton holes and neutrons both contribute to spin alignment, it does not do as well concerning the ordering of the positive-parity levels at spins $I^{\pi}=6^+-10^+$ and the distribution of $E2$ strengths connecting them. In this spin range, the calculations predict several strongly retarded $B(E2)$ values (as small as 3 mW.u.), besides the $E2$ transitions of normal size. On the basis of strong $B(E2)$ values, the favored experimental γ-ray sequence is $2^+-4^+-6_1^+-8_2^+-10_1^+$. Theoretically, strong $E2$ transitions connect the $2^+-4^+-6_2^+-8_3^+$ and $6_1^+-8_1^+-10_1^+/10_2^+$ sequences, while the 8_2^+ state would be an isomer, due to its very weak $E2$ decays of 0.1– 0.4 W.u. Obviously, the $SM1$ calculation interchanges the roles of the 6^+ yrast and yrare states. When interchanging their calculated order, the normal $E2$ strength of $B(E2,\,6_1^+\rightarrow4_1^+)=14$ W.u. would be correctly reproduced, instead of the calculated weak $B(E2,\,6_1^+\rightarrow4_1^+)=0.9$ W.u. A similar inversion relates to the ordering of the 8^+ yrast and yrare states. Both the highly retarded $B(E2,\,8_1^+\rightarrow6_1^+)$ and the large g factor of $g(8_1^+)=1.29$ typical for $\pi^{-2}(g_{9/2})$ [1] would then come out correctly. In their survey of shell model calculations in $N,\,Z<50$ nuclei within the $(g_{9/2},p_{1/2})$ model space, Rudolph *et al.* [14] pointed out that the calculations usually cannot distinguish between states of the same spin and parity whose energy distance is in the range of the mean level deviation, i.e., of the order of 250 keV in the present case.

TABLE II. Experimental and calculated $M1$ and $E2$ transitions strengths and main partitions in ^{102}Cd.

State [a]	Transition	Transition strength (W.u.)				Main partitions of initial state [b]	
		Expt.	$SM1$	$SM2$	Ref. [4]	$SM1$	$SM2$
$E2$ transitions:							
0						65% $\pi_0^{-2}\nu_0^2$	64% $\pi_0^{-2}0_1^+$
777	$2_1^+\to0_1^+$	>12.5	23	25	24	21% π_2^{-2}, 37% ν_2^4	26% $\pi_2^{-2}\,0_1^+$, 39% 2_1^+
1638	$4_1^+\to2_1^+$	>7.5	30	38	32	6% π_4^{-2}, 21% ν_4^4	35% $\pi_2^{-2}\,2_1^+$, 13% 4_1^+
2231	$6_1^+\to4_1^+$	14(1)	0.9	2.8	0.15	63% ν_6^4	49% 6_1^+
2561	$6_2^+\to4_1^+$		22	32	25	19% $\pi_2^{-2}\nu^4$, 35% ν_6^4	
							28% $\pi_4^{-2}2_1^+$, 23% $\pi_6^{-2}\,0_1^+$
2718	$8_1^+\to6_1^+$	$5.9(5)\times10^{-3}$	22	4×10^{-3}	0.12	29% $\pi_2^{-2}\nu^4$, 40% ν_8^4	
							51% $\pi_8^{-2}0_1^+$, 28% $\pi_6^{-2}2_1^+$
	$8_1^+\to 6_2^+$	1.8(2)	1.1	1.9	2.2		
3053	$8_2^+\to 6_1^+$	17(4)	0.10	26		47% π_8^{-2}	30% $\pi_2^{-2}6_1^+$, 32% 8_1^+
	$8_2^+\to6_2^+$	<14	0.44	0.12			
3578	$8_3^+\to6_1^+$		3×10^{-3}	0.23		41% ν_8^4	26% $\pi_6^{-2}2_1^+$, 11% $\pi_4^{-2}4_1^+$
	$8_3^+\to6_2^+$		27	33			
	$8_3^+\to6_3^+$		0.69	2.1			
3909	$10_1^+\to8_1^+$	2.1(7)	14.8	4.1		33% $\pi_8^{-2}\nu^4$, 40% ν^4	71% $\pi_8^{-2}\nu^4$
	$10_1^+\to8_2^+$	24(8)	0.28	0.27			
4008	$10_2^+\to8_1^+$	5.5(12)	5×10^{-3}	0.019		70% $\pi_8^{-2}\nu^2$	31% $\pi_4^{-2}\nu^4$, 18% $\pi_6^{-2}\nu^4$, 23% $\pi_2^{-2}8_1^+$
	$10_2^+\to8_2^+$	9.3(21)	0.92	20			
$M1$ transitions:							
4008	$10_2^+\to10_1^+$	0.43(10)		0.030			
4277	$11_1^+\to10_1^+$	0.17(3)	0.009	0.20		65% $\pi_8^{-2}\nu^4$	79% $\pi_8^{-2}\nu^4$
	$11_1^+\to10_2^+$	0.59(2)	0.67	7×10^{-3}			
4518	$12_1^+\to11_1^+$	0.87(8)	0.64	0.018		66% $\pi_8^{-2}\nu^4$	50% $\pi_8^{-2}\nu^4$, 9% $\pi_6^{-2}\nu^4$
5309	$13_1^+\to12_1^+$	0.16(4)	0.73	0.14		80% $\pi_8^{-2}\nu^4$	72% $\pi_8^{-2}\nu^4$, 8% $\pi_6^{-2}\nu^4$
5926	$14_1^{(+)}\to13_1^+$	>0.06	0.50	0.26		63% $\pi_8^{-2}\nu^4$	8% $\pi_8^{-2}\nu^4$, 24% $\pi_6^{-2}\nu^4$
8945	$18_1^{(-)}$					87% $\pi_{6,8}^{-2}\nu^3\nu(h_{11/2})$ [c]	
8943	$18_2^{(-)}\to17_1^{(-)}$	>0.02		5×10^{-6}			
9234	$19_1^{(-)}\to18_1^{(-)}$	>0.50	1.8	1.1			

[a]From Refs. [1–4] and the present work.

[b]$SM1$: the partition $\pi^{-2}\nu^4$ denotes two $g_{9/2}$ proton holes and up to four unpaired neutrons in the $d_{5/2}$ and/or $g_{7/2}$ orbits. $SM2$: the partition $\pi_{I'}^{-2}I_n^+$ denotes two proton holes in the $g_{9/2}$ orbit coupled to spin I', and the neutrons in the nth state of ^{104}Sn.

[c]The partition $\pi_{6,8}^{-2}\nu^3\nu(h_{11/2})$ contains one neutron in the $h_{11/2}$ orbit and three neutrons in the $d_{5/2}$ and/or $g_{7/2}$ orbits.
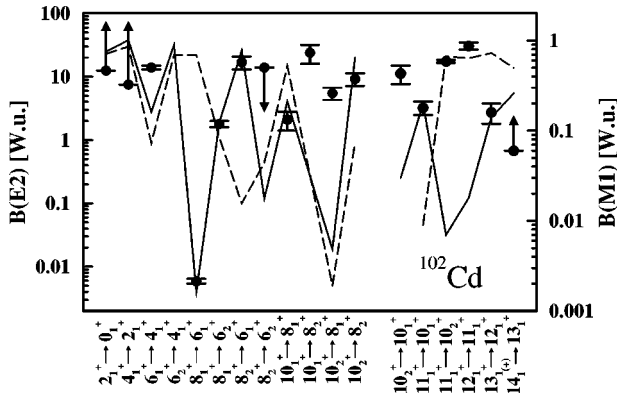

FIG. 4. Variation of the experimental $B(E2)$ and $B(M1)$ values of positive-parity transitions in comparison with the predictions of the shell model calculations $SM1$ and $SM2$ (see text).

A second shell model calculation labeled $SM2$ was performed using the single-particle states and TBME given in Refs. [18,19]. The calculated level energies are also inserted in Fig. 3, while the transition strengths and main components of the wave functions obtained in this calculation are listed in Table II. The wave functions of the lower-spin states are given in the basis $\{\pi_I^{-2}I_n^+\}$, i.e., the two $g_{9/2}$ proton holes are coupled to spin I', which then is coupled to the nth four-neutron state of spin I in ^{104}Sn. This representation highlights the parentage of the states in ^{102}Cd with respect to ^{104}Sn. For the states above spin 10^+, we used the same notation as for $SM1$. When comparing the main partitions in Table II, there are evidently pronounced similarities among the two calculations, in particular for the 2_1^+, 6_1^+, $11^+–14^+$ states, but also serious differences, for instance for the structures of the 6_2^+, 8_1^+, 8_2^+, and 10_1^+ states. In general $SM2$ reproduces the experimental $B(E2)$ better than $SM1$ does, in

particular the decays of states up to spin 8^+: note the very weak $8_1^+ \rightarrow 6_1^+$ $E2$ strength of 6 mW.u. which is nicely reproduced by $SM2$. On the other hand, the order of the 10^+ and 11^+ yrast and yrare states appears to be reversed. $SM2$ reproduces neither the large $M1$ strengths in the magnetic rotation at positive parity and spin 10–14 nor that of the $10_2^+ \rightarrow 10_1^+$ transition. Clearly, none of the shell model approaches presented is able to fit the full set of states and transition strengths in the critical spin range, which appears to be very sensitive to the shell model parameters and therefore may be very valuable for finding a better basis.

In conclusion, the doubling of states at $I^\pi = 6^+$, 8^+, and 10^+ indicates the competition of $g_{9/2}$ proton hole and neutron pair breaking at similar energies. This gives rise to retarded $E2$ strengths, besides those of normal strengths, reflecting the need to recouple both protons and neutrons in the wave functions, and may even lead to what we may call seniority isomers. The best example in ^{102}Cd is the 8^+ yrast state. Despite the rather large number of valence particles in many single-particle orbits, seniority appears to be a very good ordering parameter. None of the shell model calculations presented reproduces the order of all the yrast and yrare states and the measured distributions of $M1$ and $E2$ strengths. Above spin 10^+, spin-aligned $g_{9/2}$ proton holes and neutrons give rise to shears mode yrast configurations of the type $[\pi^{-2}(g_{9/2})_8 \nu^{2,4}(d_{5/2}, g_{7/2})]$ and strong $M1$ transitions. The present lifetime measurements fix the positive parity of this level sequence. In addition, ^{102}Cd appears to be an excellent candidate for applying the recently proposed Doppler-shift transient field technique to determine magnetic moments [20].

ACKNOWLEDGMENTS

[1] D. Alber *et al.*, Z. Phys. A **344**, 1 (1992).

[2] R. Schubart *et al.*, Phys. Scr. **T56**, 311 (1995).

[3] S. Rastikerdar, W. Gelletly, B. J. Varley, and I. S. Grant, J. Phys. G **22**, 107 (1996).

[4] J. Persson *et al.*, Nucl. Phys. **A627**, 101 (1997).

[5] A. Dewald *et al.*, Nucl. Phys. **A545**, 822 (1992).

[6] GASP Collaboration Report, INFN/Be-90/11, 1990 (unpublished).

[7] D. Kast *et al.*, Eur. Phys. J. A **3**, 115 (1998).

[8] A. Dewald, S. Harrisopulos, and P. von Brentano, Z. Phys. A **334**, 163 (1989).

[9] P. Petkov *et al.*, Nucl. Instrum. Methods Phys. Res. A **431**, 208 (1999).

[10] B. Crowell *et al.*, Phys. Rev. C **45**, 1564 (1992).

[11] G. Baldsiefen *et al.*, Nucl. Phys. **A574**, 521 (1994).

[12] S. Frauendorf and J. Reif, Nucl. Phys. **A621**, 738 (1997).

[13] H. Grawe *et al.*, Phys. Scr. **T56**, 71 (1995).

[14] D. Rudolph, K. P. Lieb, and H. Grawe, Nucl. Phys. **A597**, 298 (1996).

[15] D. Zwarts, Comput. Phys. Commun. **38**, 365 (1985).

[16] A. Jungclaus *et al.*, Nucl. Phys. **A637**, 346 (1998).

[17] A. Jungclaus *et al.*, Eur. Phys. J. A **6**, 29 (1999).

[18] M. Hjorth-Jensen, T. T. S. Kuo, and E. Osnes, Phys. Rep. **261**, 125 (1995).

[19] I. P. Johnstone and L. D. Skouras, Phys. Rev. C **51**, 2817 (1995).

[20] K. P. Lieb (unpublished).